Eur. Phys. J. A **23**, 429–434 (2005)
DOI 10.1140/epja/i2004-10091-y

THE EUROPEAN PHYSICAL JOURNAL A

Isotopic dependence of fusion probabilities for neutron-deficient and -rich colliding nuclei

R.K. Puri[a] and N.K. Dhiman

Department of Physics, Panjab University, Chandigarh-160 014, India

Received: 26 June 2004 / Revised version: 24 September 2004 /
Published online: 5 January 2005 –
Communicated by G. Orlandini

Abstract. Isotopic dependence of the fusion dynamics is studied by analyzing the collision of a large number of isotopes of Ca and Ni with $0.6 \leqslant N/Z \leqslant 2$. This study, which results from the Skyrme energy density formalism, reveals that the addition of neutrons favors fusion of reacting partners, whereas the reverse happens with the removal of neutrons. The fusion barrier heights and positions follow a non-linear second-order dependence on $\left(\frac{N}{Z}-1\right)$, whereas fusion cross-sections can be parameterized by a straight line.

PACS. 24.10.-i Nuclear reaction models and methods – 25.70.Jj Fusion and fusion-fission reactions – 25.60.Pj Fusion reactions – 25.70.-z Low and intermediate energy heavy-ion reactions

The last few years have seen a renewed interest in the field of fusion dynamics primarily due to the discovery of a large number of isotopes of different nuclei at the extreme and, subsequently, to the availability of a large number of neutron-rich and -deficient nuclear beams both in primary and secondary modes. The reactions of neutron-rich and -deficient nuclei not only provide a check for the validity of nuclear-structure models, it also enhances dramatically the possibility of synthesis of new and very neutron-rich nuclei.

Due to extensive efforts, a rich knowledge has been gathered over the neutron and proton excess domains leading to a large number of radioactive nuclear beams. One has, for example, knowledge about the properties of neutron-rich nuclei like $^{9-10}_{2}$He ($N_{\rm P}/Z_{\rm P} = 3.50$–$4.00$; $N_{\rm P}/Z_{\rm P}$ being number of neutrons/protons of the projectile), $^{26-28}_{8}$O ($N_{\rm P}/Z_{\rm P} = 2.25$–$2.50$), $^{31}_{9}$F ($N_{\rm P}/Z_{\rm P} = 2.444$), $^{34}_{10}$Ne ($N_{\rm P}/Z_{\rm P} = 2.40$), $^{30-32,37}_{11}$Na ($N_{\rm P}/Z_{\rm P} = 1.727$–$1.909$, 2.364), $^{40}_{12}$Mg ($N_{\rm P}/Z_{\rm P} = 2.333$), $^{49-51}_{18}$Ar ($N_{\rm P}/Z_{\rm P} = 1.722$–$1.833$), $^{60}_{20}$Ca ($N_{\rm P}/Z_{\rm P} = 2.0$), $^{68-78}_{28}$Ni ($N_{\rm P}/Z_{\rm P} = 1.429$–$1.786$), $^{132}_{50}$Sn ($N_{\rm P}/Z_{\rm P} = 1.64$), $^{123}_{47}$Ag ($N_{\rm P}/Z_{\rm P} = 1.617$), $^{123-128}_{48}$Cd ($N_{\rm P}/Z_{\rm P} = 1.563$–$1.667$) [1] as well as neutron-deficient (proton-rich) nuclei like $^{6}_{4}$Be ($N_{\rm P}/Z_{\rm P} = 0.50$), $^{10}_{7}$N ($N_{\rm P}/Z_{\rm P} = 0.429$), $^{12}_{8}$O ($N_{\rm P}/Z_{\rm P} = 0.50$), $^{22}_{14}$Si ($N_{\rm P}/Z_{\rm P} = 0.571$), $^{31}_{18}$Ar ($N_{\rm P}/Z_{\rm P} = 0.722$), $^{34}_{20}$Ca ($N_{\rm P}/Z_{\rm P} = 0.70$), $^{38,39}_{22}$Ti ($N_{\rm P}/Z_{\rm P} = 0.727, 0.773$), $^{45}_{26}$Fe ($N_{\rm P}/Z_{\rm P} = 0.731$), $^{48,49}_{28}$Ni ($N_{\rm P}/Z_{\rm P} = 0.714$–$0.75$), $^{54}_{30}$Zn ($N_{\rm P}/Z_{\rm P} = 0.80$), $^{217}_{92}$U ($N_{\rm P}/Z_{\rm P} = 1.359$) [2] etc. In addition, nuclear beams of a large number of neutrons as well as proton-rich nuclei are also available. Interestingly, due to several possibilities of occurrence of magic (or double magic) nuclei, isotopes of Ca and Ni are often chosen for the study of fusion dynamics [3–13]. The general limitation of these experimental attempts is that the segment of the neutron-rich/-deficient nuclei undertaken for fusion studies is rather small $\left(\frac{N}{Z} \leqslant 1.4\right)$ [9]; N/Z is the number of neutrons/protons of the compound nucleus.

Recently, we reported a systematic study of the fusion of neutron-rich colliding nuclei [13]. There, a linear isotopic dependence was predicted for the first time, that yielded a close agreement with experimental measurements reported very recently [14]. We here present, for the first time, a complete isotopic dependence of the fusion probabilities over a wide range of neutron-rich as well as -deficient colliding nuclei. As a first step, we study the collisions of different isotopes of (much sought after) Ca and Ni nuclei and present a unified formula for the role of the neutron content in the fusion probabilities. Our aim here is to investigate the effect of the addition/removal of neutrons on fusion dynamics. The present study is carried out within the framework of the Skyrme energy density model (SEDM) [15,16] that has been found to reproduce experimental data on fusion very well [17].

In the Skyrme energy density model (SEDM) [15], the nucleus-nucleus interaction potential is calculated as a difference of the energy expectation $E[= \int H(\vec{r})\mathrm{d}\vec{r}]$ of colliding nuclei at a separation distance R and at complete

[a] e-mail: rkpuri@pu.ac.in

isolation (*i.e.* at ∞)

$$V_{\rm N}(R) = E(R) - E(\infty) = \int \Big\{ H(\rho,\tau,\vec{J}) - H_1(\rho_1,\tau_1,\vec{J_1}) - H_2(\rho_2,\tau_2,\vec{J_2}) \Big\}\, {\rm d}\vec{r}, \quad (1)$$

where $H(\rho,\tau,\vec{J})$ is the Skyrme Hamiltonian density that comprises nucleonic density (ρ), kinetic energy density (τ) and spin density ($\vec{J}$). For an even-even spherical nucleus, the Hamiltonian density $H(\rho,\tau,\vec{J})$ reads as

$$\begin{aligned} &H(\rho,\tau,\vec{J}) = \\ &\frac{\hbar^2}{2m}\tau + \frac{1}{2}t_0\left[\left(1+\frac{1}{2}x_0\right)\rho^2 - \left(x_0+\frac{1}{2}\right)\left(\rho_{\rm n}^2+\rho_{\rm p}^2\right)\right] \\ &+\frac{1}{4}\left(t_1+t_2\right)\rho\tau + \frac{1}{8}\left(t_2-t_1\right)\left(\rho_{\rm n}\tau_{\rm n}+\rho_{\rm p}\tau_{\rm p}\right) \\ &+\frac{1}{16}\left(t_2-3t_1\right)\rho\nabla^2\rho + \frac{1}{32}\left(3t_1+t_2\right)\left(\rho_{\rm n}\nabla^2\rho_{\rm n}+\rho_{\rm p}\nabla^2\rho_{\rm p}\right) \\ &+\frac{1}{4}t_3\rho_{\rm n}\rho_{\rm p}\rho - \frac{1}{2}W_0\left(\rho\vec{\nabla}\cdot\vec{J}+\rho_{\rm n}\vec{\nabla}\cdot\vec{J}_{\rm n}+\rho_{\rm p}\vec{\nabla}\cdot\vec{J}_{\rm p}\right). \quad (2) \end{aligned}$$

Here n and p refer to the neutron and proton numbers, respectively. For the present analysis, Skyrme force SIII with sudden approximation is used. We apply the standard Fermi-mass density distribution [13,15,17], where, in the light of the findings of ref. [9], the neutron skin for the neutron-rich nuclei is neglected. For the details of the model, the reader is referred to refs. [13,15,17].

By adding the Coulomb potential, one can compute the total potential $V_{\rm T}(R)$ [15,17] as

$$V_{\rm T}(R) = V_{\rm N}(R) + \frac{Z_1 Z_2 e^2}{R}. \quad (3)$$

The barrier height $V_{\rm B}$ and position $R_{\rm B}$ of the reaction are, then, determined from the condition

$$\frac{{\rm d}V_{\rm T}(R)}{{\rm d}R}\Big|_{R=R_{\rm B}} = 0, \qquad \text{and} \qquad \frac{{\rm d}^2V_{\rm T}(R)}{{\rm d}R^2}\Big|_{R=R_{\rm B}} \leqslant 0. \quad (4)$$

The knowledge of the shape of the potential as well as barrier position and height, allows one to calculate the fusion probabilities [18] for incident energies above the Coulomb barrier as

$$\sigma_{\rm fus}\,({\rm mb}) = 10\pi R_{\rm B}^2\left[1-\frac{V_{\rm B}}{E_{\rm cm}}\right]. \quad (5)$$

Using the above description, we calculated the interaction potential for 115 collisions involving ^{A_1}Ca + ^{A_2}Ca, ^{A_1}Ni + ^{A_2}Ni and ^{A_1}Ca + ^{A_2}Ni; where A_1 and A_2 are the masses of isotopes involving different neutron content in the range $-0.4 \leqslant \left[\frac{N}{Z}-1\right] \leqslant 1$. We start with the collision of symmetric ($N=Z$) nuclei and then either add or remove neutrons gradually from either of the colliding pairs. In order to show the effect of addition and/or removal of the neutrons on the potential, we plot in fig. 1, the nuclear $V_{\rm N}(R)$, Coulomb $V_{\rm C}(R)$ as well as the total potential $V_{\rm T}(R)$ for illustrative examples of symmetric $^{40}_{20}$Ca$_{20}$ + $^{40}_{20}$Ca$_{20}$ and proton-rich $^{34}_{20}$Ca$_{14}$ + $^{40}_{20}$Ca$_{20}$, $^{34}_{20}$Ca$_{14}$ + $^{34}_{20}$Ca$_{14}$ as well as neutron-rich $^{40}_{20}$Ca$_{20}$ + $^{48}_{20}$Ca$_{28}$ and $^{48}_{20}$Ca$_{28}$ + $^{48}_{20}$Ca$_{28}$ colliding pairs as a function of the inter-nuclear distance R. If one looks at the nuclear potential $V_{\rm N}(R)$ in terms of the proximity concept [19] (where one can write $V_{\rm N}(R) = 2\pi\bar{R}\phi(s)$, $\phi(s)$ being the universal function), one expects a gradual shift in the potential with a change in the neutron or mass number. Naturally, due to larger relative variation in $\bar{R}$, the effect will be stronger in lighter nuclei compared to heavier ones. In other words, one should expect a stronger isotopic effect for proton-rich colliding nuclei compared to neutron-rich colliding nuclei. It is worth mentioning that the change in the neutron content not only alters the barrier heights and positions, it also changes the diffuseness of the barrier. This could have a drastic (and dramatic) effect at sub-barrier energies where one-dimensional penetration models are reported to fail to explain the measured fusion probabilities [7].

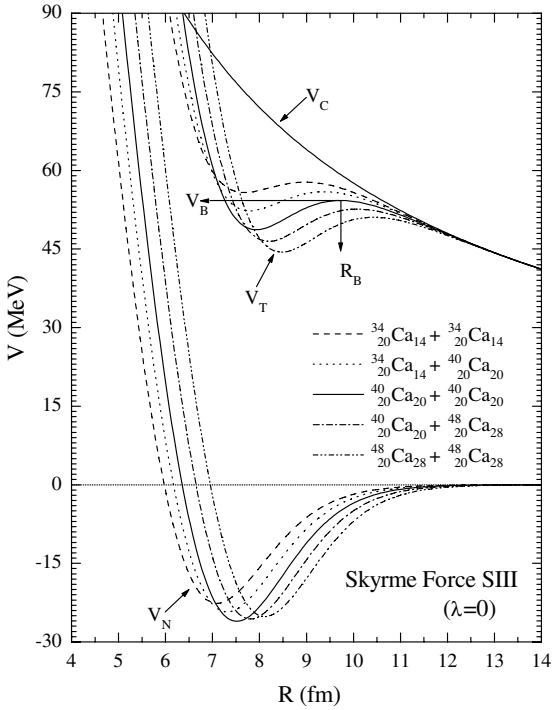

Fig. 1. The nuclear $V_{\rm N}$, Coulomb $V_{\rm C}$ and total $V_{\rm T}$ potentials for the collision of ^{34}Ca + ^{34}Ca, ^{34}Ca +^{40} Ca, ^{40}Ca + ^{40}Ca, ^{40}Ca +^{48} Ca and ^{48}Ca + ^{48}Ca as a function of the inter-nuclear distance R using the Skyrme force SIII. The fusion barrier position $R_{\rm B}$ and barrier height $V_{\rm B}$ are also indicated in one reaction.

Another point to note here is that the change in the neutron content also affects the depth of the pocket of the potential. One sees that the pocket is less deep in the collisions of proton-rich nuclei making them less favorable for fusion. One should, however, keep in mind that the sudden approximation, used in the present analysis, is not a good assumption in the interior parts of the potential.

Before, we present the systematic study of the effect of the neutron content on fusion, let us compare our results (for the isotopic dependence of the fusion barriers) with

Table 1. Fusion barrier heights V_B and positions R_B using the Skyrme force SIII along with other theoretical and experimental data.

Sr. No.	Reaction	$Z_1 \cdot Z_2$	$A_1^{1/3}+A_2^{1/3}$	SEDM SIII		S_B (fm)	Expt.		Theoretical Results	
				V_B (MeV)	R_B (fm)		V_B (MeV)	R_B (fm)	V_B (MeV)	R_B (fm)
1.	$^{40}Ca + {}^{40}Ca$	400	6.84	54.3	9.73±0.05	2.03	52.30±0.5	8.8±0.5 [10]	55.9 [10]	–
							50.60±2.8	9.50±0.5 [17]	54.9 [10]	–
							55.60±0.8	9.10±0.6 [17]	57.76	9.25 [20]
									55.92	9.50 [21]
									58.01	9.2 [22]
									55.03	9.742 [24]
2.	$^{40}Ca + {}^{44}Ca$	400	6.95	53.4	9.92±0.05	2.09	51.70±1.2	8.50±0.5 [10]	52.4 [23]	–
									55.0 [10]	–
									54.0 [10]	–
									54.35	9.877 [24]
3.	$^{40}Ca + {}^{48}Ca$	400	7.05	52.6	10.06±0.05	2.10	53.2	10.08 [9]	54.3 [10]	
							51.30±1.0	7.80±0.3 [10]	53.2 [10]	
									56.05	9.60 [20]
									54.31	9.80 [21]
									56.52	9.5 [22]
									54.08	9.931 [24]
4.	$^{48}Ca + {}^{48}Ca$	400	7.27	51.1	10.40±0.10	2.17	51.7	10.38 [9]	54.58	9.90 [20]
									53.22	10.10 [21]
5.	$^{40}Ca + {}^{58}Ni$	560	7.29	73.2	10.07±0.05	1.82	73.0	9.6±0.3 [8]	75.7	9.80 [8]
							73.36	10.20 [25]	74.75	9.89 [25]
									76.37	9.75 [25]
									75.47	9.80 [25]
									74.72	10.05 [25]
									73.57	10.31 [25]
6.	$^{40}Ca + {}^{62}Ni$	560	7.38	72.3	10.19±0.10	1.83	71.0	9.5±0.2 [8]	75.2	9.9 [8]
							72.30	10.35 [25]	73.89	10.02 [25]
									75.39	9.89 [25]
									74.54	9.90 [25]
									73.64	10.20 [25]
									72.87	10.42 [25]
7.	$^{58}Ni + {}^{58}Ni$	784	7.74	99.0	10.26±0.10	1.46	97.90	8.30 [4]	99.0	8.8 [3]
									104.5	10.03 [5]
									95.6 [23]	–
8.	$^{58}Ni + {}^{64}Ni$	784	7.87	97.3	10.56±0.05	1.60	96.0	8.20 [4]	102.8	10.23 [5]
									94.1 [23]	–
9.	$^{64}Ni + {}^{64}Ni$	784	8.00	95.7	10.82±0.10	1.70	93.50	8.60 [4]	101.1	10.42 [5]

experimental as well as with other theoretical results. In table 1, we list the isotopes of colliding Ca/Ni nuclei along with the fusion barrier heights and positions. We also list the fusion surface distance $S_B = R_B - (R_1 + R_2)$. The different theoretical results listed in the table are based on several different descriptions. For example, ref. [3] used the Krappe-Nix-Sierk formula for ion-ion potentials, whereas results of ref. [5] are based on the concept of transmission across a mildly absorptive effective fusion barrier. Results reported in refs. [20,21] are based on the Skyrme energy density formalism, whereas ref. [22] is based on the Brueckner energy density formalism. The coupled channel technique was used in refs. [23,24], whereas ref. [25] , is a compilation of several of the above-mentioned methods.

As evident from the table, one can divide the reactions into two categories: i) the symmetric colliding nuclei $X + X$; X being either Ca or Ni isotope and ii) the cross-reacting partners involving Ca and Ni nuclei. One can observe several visible conclusions: i) our present results with the Skyrme force SIII are the closest compared to all other reported theoretical results, which gives us confidence in the model. ii) All theoretical models and experimental measurements give smaller reduced barrier heights with the addition of neutrons. iii) Though all the theoretical models predict shifting of the barrier outward with the addition of neutrons, some controversial results can be seen in the experimental measurements. For example, one experimental measurement listed the barrier position R_B in $^{40}Ca + {}^{48}Ca = 7.8 \pm 0.3$ fm [10], whereas other recent measurement extracted $R_B = 10.08$ fm [9]. These controversies need to be sorted out before the isotopic dependence trend can be studied experimentally. If one looks the

fusion surface distance $S_{\rm B}$, one finds that it decreases with the product of the charges for nearly symmetric cases. This is because of the fact that one needs more penetration to counterbalance the Coulomb force in heavier colliding nuclei compared to the lighter one. Interestingly, for a given pair, $S_{\rm B}$ increases with the neutron content. This happens because while the product of the charges stays constant, the contribution of nuclear interaction increases with addition of neutrons that allows the barrier to occur at larger distances. From the table, one also realizes that the range of the experimentally measured isotopic dependence of fusion probabilities is very limited $\left(\frac{N}{Z} \leqslant 1.4\right)$.

In order to reach a meaningful understanding and conclusion, we calculate the fusion barrier heights and positions for 115 reactions involving the isotopes of Ca and Ni with $0.6 \leqslant N/Z \leqslant 2.0$ and analyze the normalized variation in the barrier heights and positions over a $N = Z$ colliding pair as

$$\Delta R_{\rm B}(\%) = \frac{R_{\rm B} - R_{\rm B}^0}{R_{\rm B}^0} \times 100, \tag{6}$$

$$\Delta V_{\rm B}(\%) = \frac{V_{\rm B} - V_{\rm B}^0}{V_{\rm B}^0} \times 100, \tag{7}$$

where $R_{\rm B}^0$ and $V_{\rm B}^0$ are, respectively, the positions and heights of the barriers for a $N = Z$ symmetric colliding pair.

Similarly, one can also define the normalized fusion cross-section:

$$\Delta\sigma_{\rm fus}(\%) = \frac{\sigma_{\rm fus}(E_{\rm cm}^0) - \sigma_{\rm fus}^0(E_{\rm cm}^0)}{\sigma_{\rm fus}^0(E_{\rm cm}^0)} \times 100 \tag{8}$$

with $E_{\rm cm}^0$ and $\sigma_{\rm fus}^0$ being the center-of-mass energy and fusion cross-section for a symmetric colliding pair. The advantage of such normalized quantities is that these quantities give a mass-independent picture. In fig. 2, we plot $\Delta R_{\rm B}(\%)$ (upper part) and $\Delta V_{\rm B}(\%)$ (lower part) as a function of $\left(\frac{N}{Z} - 1\right)$. The addition of neutrons extends the $R_{\rm B}$ toward larger distances monotonically whereas $V_{\rm B}$ decreases linearly. The extended barrier positions should give reduced barrier heights. One sees a reverse trend in the case of neutron-deficient colliding nuclei. In addition, the variation in the barrier positions and heights is stronger in proton-rich colliding nuclei compared to neutron-rich colliding nuclei.

The neutron-rich and -deficient cases can be parameterized separately by a straight line as

$$\Delta R_{\rm B}(\%) = \begin{cases} 19\left[\frac{N}{Z} - 1\right] & \frac{N}{Z} \geqslant 1, \\ 27\left[\frac{N}{Z} - 1\right] & \frac{N}{Z} \leqslant 1, \end{cases} \tag{9}$$

$$\Delta V_{\rm B}(\%) = \begin{cases} -14.5\left[\frac{N}{Z} - 1\right] & \frac{N}{Z} \geqslant 1, \\ -23\left[\frac{N}{Z} - 1\right] & \frac{N}{Z} \leqslant 1. \end{cases} \tag{10}$$

These different variations of $\Delta R_{\rm B}(\%)$ and $\Delta V_{\rm B}(\%)$ for the $N/Z \geqslant 1$ and $N/Z \leqslant 1$ cases, compels us to choose a new unified non-linear functional valid for both cases. The unified formula for $-0.4 \leqslant \frac{N}{Z} - 1 \leqslant 1$ can be written as

$$\begin{aligned} \Delta R_{\rm B}(\%) &= 24\left(\tfrac{N}{Z} - 1\right) - 6.2\left(\tfrac{N}{Z} - 1\right)^2, \\ \Delta V_{\rm B}(\%) &= -18.5\left(\tfrac{N}{Z} - 1\right) + 6\left(\tfrac{N}{Z} - 1\right)^2. \end{aligned} \tag{11}$$

We see from fig. 2 that our above formulae are able to reproduce the exact values quite closely. The second-order non-linear term in the above equations takes care of the different dependences for $\frac{N}{Z} \geqslant 1$ and $\frac{N}{Z} \leqslant 1$. We also display in the figure, the available results of other theoretical models as well as experimental measurements. In, all the cases, where values of fusion barrier positions and heights for a $N/Z = 1$ colliding pair are not available, a straight-line interpolation is used between the known points to get $\Delta R_{\rm B}(\%)$ and $\Delta V_{\rm B}(\%)$. We see that our present results fall on the top of these results. From the figure, it is also clear that there is a monotonic reduction in the fusion probabilities for proton-rich colliding nuclei, whereas an enhancement can be seen for the neutron-rich colliding pairs.

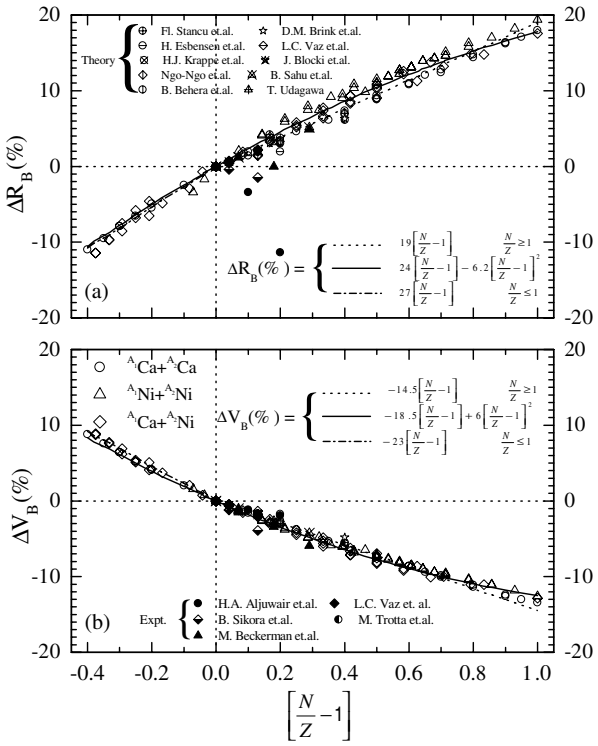

Fig. 2. The normalized barrier positions $\Delta R_{\rm B}(\%)$ and barrier heights $\Delta V_{\rm B}(\%)$ as a function of $\left(\frac{N}{Z} - 1\right)$. We display the results of our calculations for the collisions of ^{A_1}Ca + ^{A_2}Ca, ^{A_1}Ca + ^{A_2}Ni and ^{A_1}Ni + ^{A_2}Ni along with other available theoretical and experimental values (see table 1). In all those cases where no data are available for the $N = Z$ case, a straight line interpolation is used to extract $\Delta R_{\rm B}(\%)$ and $\Delta V_{\rm B}(\%)$. The dotted and dash-dotted lines are the fits over the calculated points, respectively, for $N/Z > 1$ and $N/Z < 1$, whereas the solid line represents the fit for the full range, *i.e.* $-0.4 \leqslant \left[\frac{N}{Z} - 1\right] \leqslant 1$. The theoretical data reported here are taken from ref. [25].

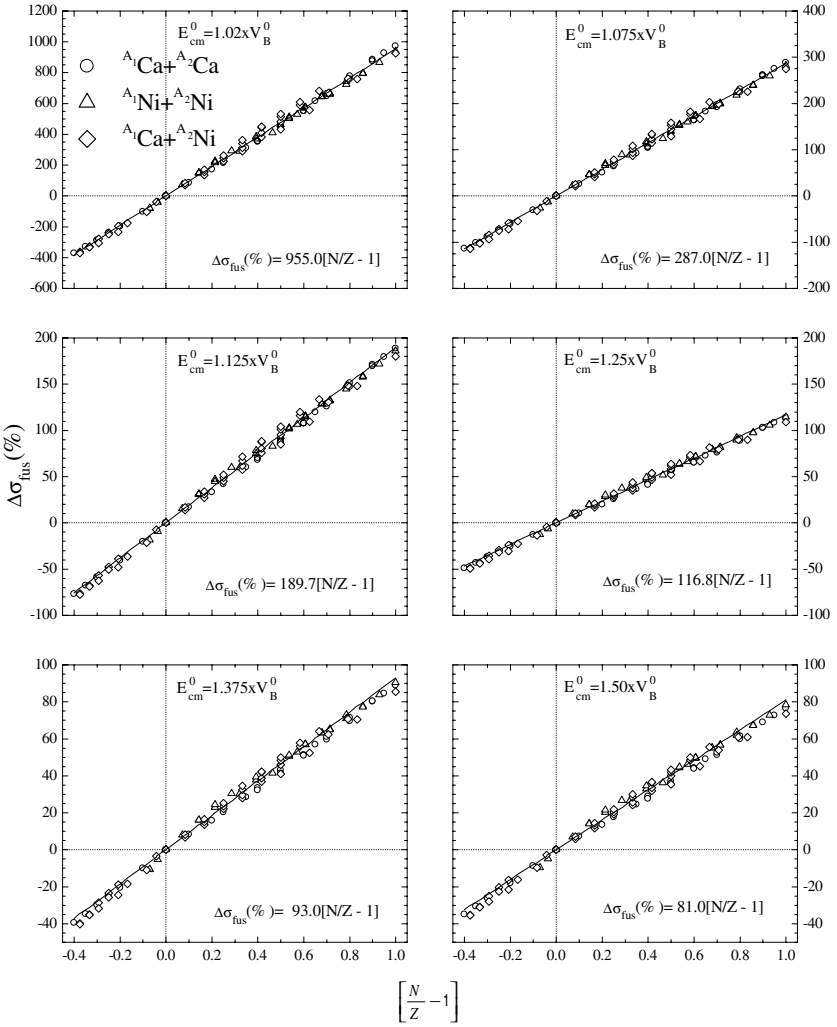

Fig. 3. The normalized fusion cross-section $\Delta\sigma_{\rm fus}(\%)$ as a function of $\left(\frac{N}{Z}-1\right)$ for the collisions of ^{A_1}Ca + ^{A_2}Ca, ^{A_1}Ni + ^{A_2}Ni and ^{A_1}Ca + ^{A_2}Ni at incident energies $E_{\rm cm} = 1.02V_{\rm B}^0$, $1.075V_{\rm B}^0$, $1.125V_{\rm B}^0$, $1.25V_{\rm B}^0$, $1.375V_{\rm B}^0$ and $1.5V_{\rm B}^0$. The available experimental data are also displayed.

In fig. 3, we display the $\Delta\sigma_{\rm fus}(\%)$ as a function of $\left(\frac{N}{Z}-1\right)$ for all three series at different center-of-mass energies $E_{\rm cm}$. We see that all fusion cross-sections can be parameterized by a single linear function of the form

$$\Delta\sigma_{\rm fus}(\%) = \alpha\left[\frac{N}{Z}-1\right], \qquad (12)$$

where α depends on the center-of-mass energy. One can also make a couple of additional observations: i) Though $\Delta R_{\rm B}(\%)$ and $\Delta V_{\rm B}(\%)$ need a second-order non-linear parameterization, $\Delta\sigma_{\rm fus}(\%)$ can be parameterized by a first-order straight line. This happens because the stronger variation of $\Delta R_{\rm B}(\%)$ in neutron-deficient colliding nuclei is counterbalanced by the corresponding $\Delta V_{\rm B}(\%)$ variation; therefore, the net variation in the fusion cross-section follows a straight line. ii) The parameter α in eq. (12) is much stronger for the near-barrier incident energies which reduce to an insignificant level for very high incident energies. Similar observations are also made by other authors [3–12]. This clearly indicates that the role of the neutron content is limited to near-barrier incident energies, therefore, the processes that happen around the Coulomb barrier can be expected to be affected by the variation in the neutron content.

Summarizing, we presented a complete analysis of the isotopic dependence of the fusion probabilities for neutron-rich as well as neutron-deficient colliding nuclei using the Skyrme energy density model. We observed a non-linear second-order isotopic dependence for the normalized variation in the barrier heights and positions with the neutron content. The fusion probabilities, however, show a linear isotopic dependence for the entire range of the neutron-rich and -deficient cases. Our results are in good agreement with other (limited) available experimental data as well as with other theoretical models. Experiments are needed to verify our predictions.

References

1. S.M. Lukyanov *et al.*, J. Phys. G **28**, L41 (2002); A. Leistenschneider *et al.*, Phys. Rev. Lett. **86**, 5442 (2001); S. Aoyama, K. Kato, K. Ikeda, Phys. Rev. C **55**, 2379 (1997); T. Suzuki *et al.*, Phys. Rev. Lett. **75**, 3241 (1995); L. Weissman *et al.*, Phys. Rev. C **67**, 054314 (2003); T. Ishii *et al.*, Eur. Phys. J. A **13**, 15 (2002); H. Scheit *et al.*, Phys. Rev. C **63**, 014604 (2001).
2. O.N. Malyshev *et al.*, Eur. Phys. J. A **8**, 295 (2000); J. Giovinazzo *et al.*, Eur. Phys. J. A **10**, 73 (2001); A. Lépine-Szily *et al.*, Phys. Rev. C **65**, 054318 (2002); B. Blank *et al.*, Phys. Rev. C **54**, 572 (1996).
3. C.E. Aguiar *et al.*, Nucl. Phys. A **500**, 195 (1989).
4. M. Beckerman *et al.*, Phys. Rev. C **25**, 837 (1982).
5. Basudeb Sahu *et al.*, Phys. Rev. C **57**, 1853 (1998).
6. R.K. Puri, N.K. Dhiman, *Proceedings of the DAE Symposium*, Vol. **46B** (2003) p. 268.
7. C.L. Jiang *et al.*, Phys. Rev. Lett. **89**, 052701 (2002).
8. B. Sikora *et al.*, Phys. Rev. C **20**, 2219 (1979).
9. M. Trotta *et al.*, Phys. Rev. C **65**, 011601(R) (2001).
10. H.A. Aljuwair *et al.*, Phys. Rev. C **30**, 1223 (1984).
11. V.I. Zagrebaev, Phys. Rev. C **67**, 061601(R) (2003).
12. U. Jahnke *et al.*, Phys. Rev. Lett. **48**, 17 (1982).
13. R.K. Puri, M.K. Sharma, R.K. Gupta, Eur. Phys. J. A **3**, 277 (1998).
14. K.E. Zyrormski *et al.*, Phys. Rev. C **63**, 024615 (2001).
15. R.K. Puri, P. Chattopadhyay, R.K. Gupta, Phys. Rev. C **43**, 315 (1991).
16. D. Vautherin, D.M. Brink, Phys. Rev. C **5**, 626 (1972).
17. R.K. Puri, R.K. Gupta, Phys. Rev. C **45**, 1837 (1992).
18. C.Y. Wong, Phys. Lett. B **32**, 567 (1970); **42**, 186 (1972); Phys. Rev. Lett. **31**, 766 (1973).
19. J. Blocki *et al.*, Ann. Phys. (N.Y.) **105**, 427 (1977).
20. Fl. Stancu, D.M. Brink, Nucl. Phys. A **270**, 236 (1976).
21. D.M. Brink, Fl. Stancu, Nucl. Phys. A **299**, 321 (1978).
22. B. Behera, K.C. Panda, R.K. Satpathy, Phys. Rev. C **20**, 683 (1979).
23. T. Udagawa, Phys. Rev. C **32**, 124 (1985).
24. H. Esbensen, S.H. Fricke, S. Landowne, Phys. Rev. C **40**, 2046 (1989).
25. L.C. Vaz, J.M. Alexander, G.R. Satchler, Phys. Rep. **69**, 373 (1981).